Undergraduate Journal of Experimental Microbiology and Immunology (UJEMI) Vol. 24:1-12
Copyright © September 2019, M&I UBC

Developed biofilm assay suggests *Escherichia coli* Nissle 1917 may mediate biofilm inhibition in *Escherichia coli* K-12 in liquid co-culture

Alex Fung, Anderson Li, Helen Lin, Vivian Li

Department of Microbiology and Immunology, University of British Columbia, Vancouver, British Columbia, Canada

SUMMARY *Escherichia coli* K12 (K12) is a bacterial species known to form biofilm, which is a community of bacteria residing in a matrix of secreted polysaccharides and proteins. This leads to reduced efficacy in conventional antibiotic regimens, and may cause chronic infections in patients. *Escherichia coli* Nissle 1917 (EcN), a probiotic strain, has been shown to decrease biofilm formation of co-cultured strains of *Escherichia coli* (*E. coli*); however, this mechanism is not well understood. We hypothesize that EcN mediated inhibition of biofilm formation of co-cultured *E. coli* strains involves the CpxA/CpxR two-component signaling system in the Cpx pathway which inhibits biofilm formation. Thus, we expect that when EcN is co-cultured with *E. coli* strain K12, biofilm formation will be reduced. CpxA indirectly deactivates the Cpx pathway, whereas CpxR activates the Cpx pathway. By using genetic knockouts of *cpxR* and *cpxA,* we expect to see that a Δ*cpxR* knockout will show increased biofilm formation, while a Δ*cpxA* knockout will show reduced biofilm formation. Here, we demonstrate that EcN may have inhibitory effects on the development of K12 biofilm in liquid co-cultures. This was determined by quantifying and comparing crystal violet stains of biofilm formation at the air-liquid-solid interface in glass test tubes, which is shown here to enhance biofilm formation. Although the findings were not conclusive to address our original hypothesis, our results led to the development of a biofilm assay for direct detection and quantification of biofilm formation, laying the groundwork for future experiments.

INTRODUCTION

Escherichia coli (*E. coli*) are found either as planktonic free swimming bacteria, or as a non-motile clustering of bacteria referred to as a biofilm (1). Biofilms, in addition to sessile bacterial cells, are made of extracellular polymeric substances consisting of bacterially secreted polysaccharides, nucleic acids and proteins (1 - 3). Biofilms are involved in many chronic infections due to the extracellular matrix providing bacterial cells increased tolerance to antibiotics and disinfectants (1, 4). This creates challenges in health settings since pathogenic biofilms can persist on surfaces of medical equipment and in organ lumen, causing infections (1, 2). Planktonic bacteria transition to biofilm formation when a change is detected in the environment, such as encountering a nutrient rich surface within a nutrient poor environment (4). These changes in nutrient concentrations are detected through various two-component signaling systems, such as CpxA/CpxR in the Cpx pathway (4, 5). Activation of the Cpx pathway can repress genes such as flagella expression, facilitating transitioning from a motile to sessile state (4). This adhesion stage is then further regulated by non-specific binding dependent on the abiotic surface or by specific receptors binding to biotic surfaces (6). Once the cells adhere to the surface, three-dimensional structures begin to form through secretion of substrates by bacteria ensuring a cohesive and mature biofilm (6).

The regulation of *E. coli* biofilms is found to involve many factors. Some downregulate amyloid curli fibers and cellulose, which are involved in adhesion and the biofilm matrix (7). Another factor is when CpxA detects stress in the environment and activates CpxR in the Cpx pathway, leading to biofilm inhibition (5 - 8) (Fig. 1). This pathway is, in turn, regulated by DegP (8, 9), which is a protease within the periplasm of *E. coli* (10). Mutations in DegP have demonstrated its ability to trigger the proteolysis of CpxP, an inhibitor of the

Published Online: 6 September 2019

Citation: Fung A, Li A, Lin H, Li V. 2019. Developed biofilm assay suggests *Escherichia coli* Nissle 1917 may mediate biofilm inhibition in *Escherichia coli* K-12 in liquid co-culture. UJEMI 24:1-12

Editor: Julia Huggins, University of British Columbia

Copyright: © 2019 Undergraduate Journal of Experimental Microbiology and Immunology. All Rights Reserved.

Address correspondence to: https://jemi.microbiology.ubc.ca/

Cpx pathway (8, 9). DegP has also been implicated in the degradation of misfolded proteins and other outer membrane proteins within the periplasm, and is shown to be critical to the survival of *E. coli* at high temperatures (10, 11). Furthermore, DegP has been shown to be involved in inhibition of the Cpx-mediated type III secretion processes of enteropathogenic *E. coli* (12), which are involved in cell motility. A recent study has further shown that the addition of DegP into growth media is sufficient to inhibit biofilm formation of an enterohemorrhagic *E. coli* strain (EHEC) (13). However, the mechanism of interaction of DegP with bacteria outside of the periplasm is not well understood. Biofilm formation can also be influenced by the presence of other bacteria in the environment. In co-culture studies, secretions by other bacteria may inhibit biofilm formation through processes such as downregulation of adhesins, and degradation of quorum sensing factors and structural matrix components (6).

Although the mechanism involved in biofilm inhibition through the addition of DegP is not well understood, we propose it is due to the ability of extracellular DegP to regulate the Cpx pathway (Fig. 1). It has also been demonstrated that co-culturing EHEC with *E. coli* Nissle 1917 (EcN) reduces biofilm formation in EHEC (13). EcN is one of the strains of *E. coli* that has demonstrated its ability to produce extracellular DegP (13). Thus, we expect that when EcN is co-cultured with *E. coli* K-12 MG1655 (K12), biofilm formation in K12 will also be reduced (Fig. 2). Furthermore, we hypothesis that a co-culture of EcN and *E. coli* K-12 JW3883-1 *cpxR* knockout strain (Δ*cpxR*), and a monoculture of Δ*cpxR* will show no reduction in biofilm when compared to K12 (Fig. 3). In contrast, the *E. coli* K-12 JW3882-1 *cpxA* knockout strain (Δ*cpxA*) has been shown to increase CpxR activation due to a cross-talk mechanism with another two-component system in *E. coli* (14). Thus, a co-culture of EcN and Δ*cpxA*, and a monoculture of Δ*cpxA* will show a reduction in biofilm formation, when compared to K12, because of cross-talk that activates CpxR to inhibit biofilm formation (Fig. 4). We expect these observations in our experiment as we hypothesize that extracellular DegP secreted by EcN will activate the Cpx pathway, hindering biofilm formation. However, if *cpxR* is knocked out, this pathway will no longer function, leading to the loss of biofilm inhibition, resulting in the observation of biofilm formation. If *cpxA* is knocked out, CpxR will have increased expression compared to WT levels, leading to the absence of biofilm. Strains will be grown on glass, polystyrene and polypropylene surfaces and in different media as previous work has demonstrated that multiple changes in physicochemical and environmental conditions cause variations in biofilm expression (15).

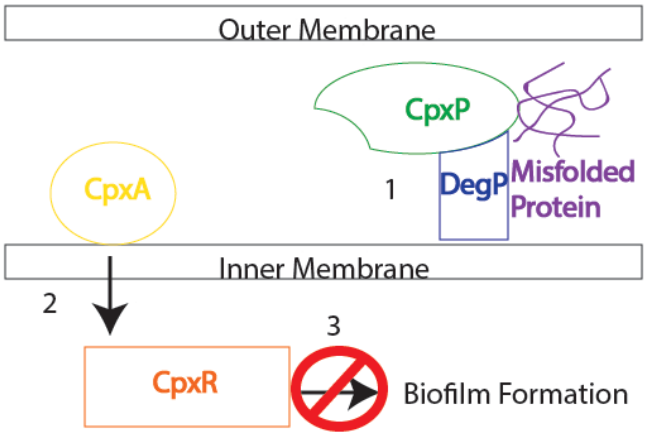

FIG. 1 Inactivated Cpx pathway promotes biofilm formation. Activated Cpx pathway inhibits biofilm formation. (1) In the presence of misfolded protein, CpxP binds to it and the complex is degraded by a protease, DegP. (2) CpxA can now activate CpxR causing (3) biofilm formation to be inhibited.

METHODS AND MATERIALS

Bacterial strains and growth conditions. *E. coli* MG1655 WT strain (K12) and *E. coli* Nissle 1917 (EcN) were obtained from the University of British Columbia, from the laboratory stocks of the Department of Microbiology and Immunology and as gift from the Finlay Laboratory, respectively. Strains *E. coli* JW3882-1 *cpxA* knockout (Δ*cpxA*) and *E. coli* JW3883-1 *cpxR* knockout (Δ*cpxR*) were obtained from the Coli Genetic Stock Centre (CGSC). Both Δ*cpxA* and Δ*cpxR* contained a genomically encoded kanamycin resistance cassette which replaced the target genes. The *E. coli* K12 and EcN strains were propagated on Lysogeny Broth (LB) agar plates, and Δ*cpxA* and Δ*cpxR* were propagated on LB agar plates supplemented with kanamycin at a concentration of 50 µg/mL. All strains were grown at 37°C with aeration.

Strain genotype confirmation. To confirm the identity of the Δ*cpxA* and Δ*cpxR* strains, colony PCR and agarose gel electrophoresis were performed, followed by sequence confirmation with Sanger Sequencing through the UBC NAPS (Nucleic Acid Protein Service) unit. The two oligonucleotide primer pairs for PCR were designed to flank the *cpxA* and *cpxR* genes, amplifying the region containing the kanamycin resistance cassette (Table S1 in the supplementary material).

Both forward and reverse primer pairs were designed using SnapGene® software, and were ordered from Integrated DNA Technologies®. Each PCR reaction contained 5 µL of 10x Taq buffer with (NH4)2SO4, 2µL of 50 mM MgCl2, 1 µL of 10 mM dNTPs, 0.5 µL of 1% DMSO, 0.4 µL of Taq polymerase (Thermo Fisher, catalogue #10342020), 35.1 µL of deionized water, 1 µL each of the forward and reverse primers for each strain from the 100 µM stock concentrations, and a single plate-isolated colony from each respective strain was added into the reaction using a sterile pipette tip. Two positive controls were included using K12 plate-isolated colonies and both CpxA and CpxR primers. One no-template negative control was also included. PCR was performed in the BioRad T100TM Thermal Cycler. The reaction was initiated with 3 min at 95°C (denaturation). Afterwards, 30 cycles were carried out with the following protocol: 95°C for 60 s (denaturation), followed by 55°C for 60 s (annealing), and then 72°C for 60 s (extension) followed by a final extension at 72°C for 10 min. The PCR products (10 µL of each) were loaded on a 1% agarose gel containing SYBR® Safe DNA gel stain in 1X TBE buffer (Invitrogen) with 2 µL of 6X BlueJuice™

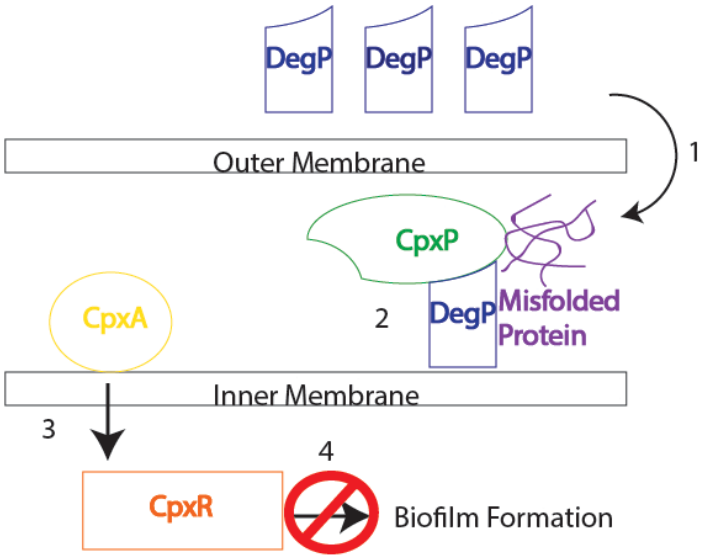

FIG. 2 EcN releases DegP which is hypothesized to be taken up by *E. coli* and can activate the Cpx pathway. (1) DegP enters the periplasm of *E. coli* where (2) it degrades CpxP. (3) CpxA is no longer inactivated by CpxP and can now activate CpxR causing (4) biofilm inhibition.

Gel Loading Buffer (Invitrogen). DNA gel electrophoresis was run at 100V for 80 min. Amplicons were visualized and imaged with UV light using AlphaImager® (ProteinSimple), purified using the PureLink™ PCR Purification Kit (Invitrogen), and subsequently sent to the UBC NAPS unit for Sanger Sequencing with the primers listed in Supplementary Table S1.

Growth curve analysis. Overnight cultures of K12, EcN, Δ*cpxA* and Δ*cpxR* (each in 3 mL LB) were diluted in LB to a common OD600 value of 0.02 (1.6 x 10^7 cells/mL) and 200 µL (per well) of each were subsequently transferred to a flat-bottom Corning™ Clear Polystyrene 96-Well Microplate (ThermoFisher) in three biological replicates. Plates were incubated at 37°C with shaking at 567 rpm for three seconds every 10 mins in a microplate reader (Synergy H1 Hybrid Multi-Mode Reader; BioTek) over a 16 h period, with OD600 readings measured every 10 min.

Preparation of 0.1% crystal violet solution. A stock solution of 1% crystal violet was prepared by combining 0.5 g of crystal violet powder with 5 mL of 100% ethanol and 44.5 mL of deionized water. It was then diluted to 0.1% crystal violet solution by adding 1 mL of 1% stock crystal violet stock solution to 0.9 mL of ethanol and 8.1 mL of deionized water as required.

Biofilm formation in 96 well plates. Overnight bacterial cultures of K12, EcN, Δ*cpxA*, and Δ*cpxR* were diluted to a common OD600 of 0.05, which were then used to inoculate one 96-well plate in monocultures of K12, EcN, Δ*cpxA,* and Δ*cpxR*; and co-cultures of K12 and EcN, Δ*cpxA* and EcN, and Δ*cpxR* and EcN. Following incubation for various durations (Fig. S1), the wells were washed with water and stained with 0.1% crystal violet solution. Subsequently, biofilm formed inside the wells were eluted with 30% acetic acid, and all well contents were transferred to a new 96-well plate for quantification of biofilm by measuring the A590 value.

Assessing EcN-mediated biofilm inhibition at the air-liquid-solid interface in glass test tubes. Plate-isolated colonies of K12, EcN, Δ*cpxA* and Δ*cpxR* were inoculated in 1 mL of LB in loosely-capped glass test tubes, to generate monocultures of K12, EcN, Δ*cpxA* and Δ*cpxR*, and co-cultures of EcN and K12, EcN and Δ*cpxA*, and EcN and Δ*cpxR,* which were all incubated at 30°C without shaking for 72 h. Three biological replicates were performed.

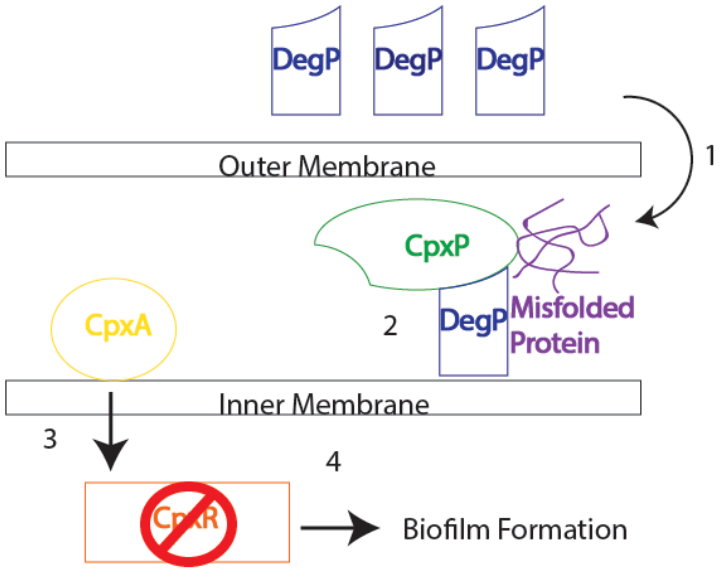

FIG. 3 Absence of CpxR (Δ*cpxR*) promotes biofilm formation. (1) DegP enters the periplasm of *E. coli* where (2) it degrades CpxP. (3) Though CpxA is activated, CpxR is not present in cells; thus, (4) biofilm formation cannot be inhibited.

Following incubation, the planktonic cells from each set of replicates were removed with a pipette, pooled, and the OD600 reading was measured using the microplate spectrophotometer (Epoch; BioTek). A LB-only negative control was included. The test tubes were rinsed three times with deionized water and allowed to air dry upside down for three hours at room temperature. The biofilms were then stained with 2 mL of 0.1% crystal violet solution in each tube, and allowed to rest for 15 min at room temperature. The stain was subsequently removed and the tubes were washed five times with deionized water, and dried upside down overnight at room temperature. On the following day, the crystal violet was eluted with 2 mL of 95% ethanol at room temperature for 30 min, followed by a transfer of 200 µL from each tube into a new 96-well plate for the A590 reading to be determined using the microplate spectrophotometer (Epoch; BioTek). A negative control was included by using a LB-only tube which underwent the same staining process.

RESULTS

Strain verification and growth curves for strain characterization of *E. coli* K-12, *E. coli* K-12 Δ*cpxA*, and *E. coli* K-12 Δ*cpxR*. *E. coli* K-12 Δ*cpxA* (Δ*cpxA*) and *E. coli* K-12 Δ*cpxR (*Δ*cpxR*) are both cultivated *E. coli* K-12 strains with kanamycin cassettes inserted to disrupt the respective genes. PCR results for the mutant strains yielded single bands (Fig. S2). The PCR products were purified, and Sanger Sequencing confirmed the correct identity for each mutant.

Once verified, 16 h growth curves for *E. coli* K-12 (K12), EcN, Δ*cpxA*, and Δ*cpxR* were generated to ensure that all four strains exhibited similar growth rates so that results obtained from downstream experiments would not need to be normalized for differences in growth rates. All growth curves generated entered the exponential phase of growth at approximately 2 h and displayed a similar growth pattern (Fig. 5). At the end of the 16 h incubation, the OD_{600} values for K12, EcN, Δ*cpxA*, Δ*cpxR* are 1.127, 0.702, 0.936, and 0.842, respectively (Fig. 5). Despite these differences, we decided to continue with no adjustments as all strains exhibited similar exponential phase growth.

Optimization of growth conditions in 96-well plates showed inconsistent biofilm formation. In order to optimize conditions for biofilm formation and subsequent quantification, a number of growth conditions in polystyrene 96-well plates were tested,

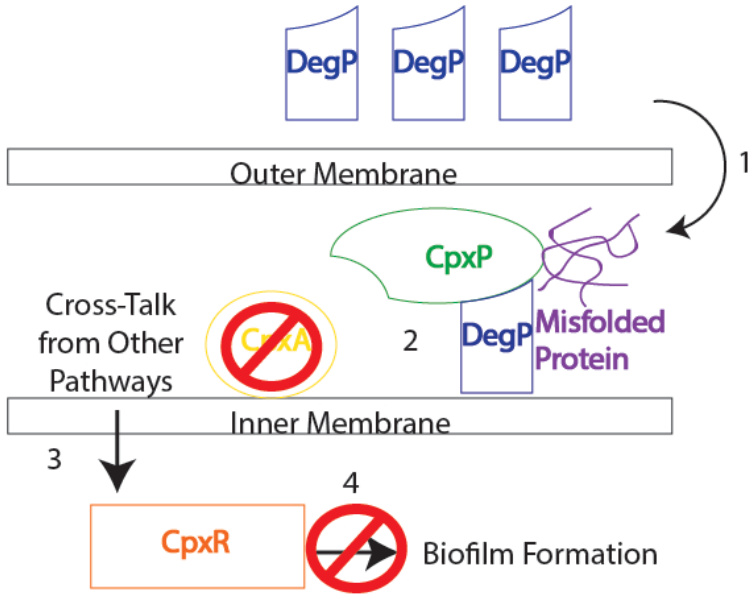

FIG. 4 Absence of CpxA (Δ*cpxR*) allows cross-talk between other pathways leading to biofilm inhibition. (1) DegP enters the periplasm of *E. coli* where (2) it degrades CpxP. (3) Absence of CpxA allows activation of CpxR through other signalling pathways causing (4) biofilm inhibition.

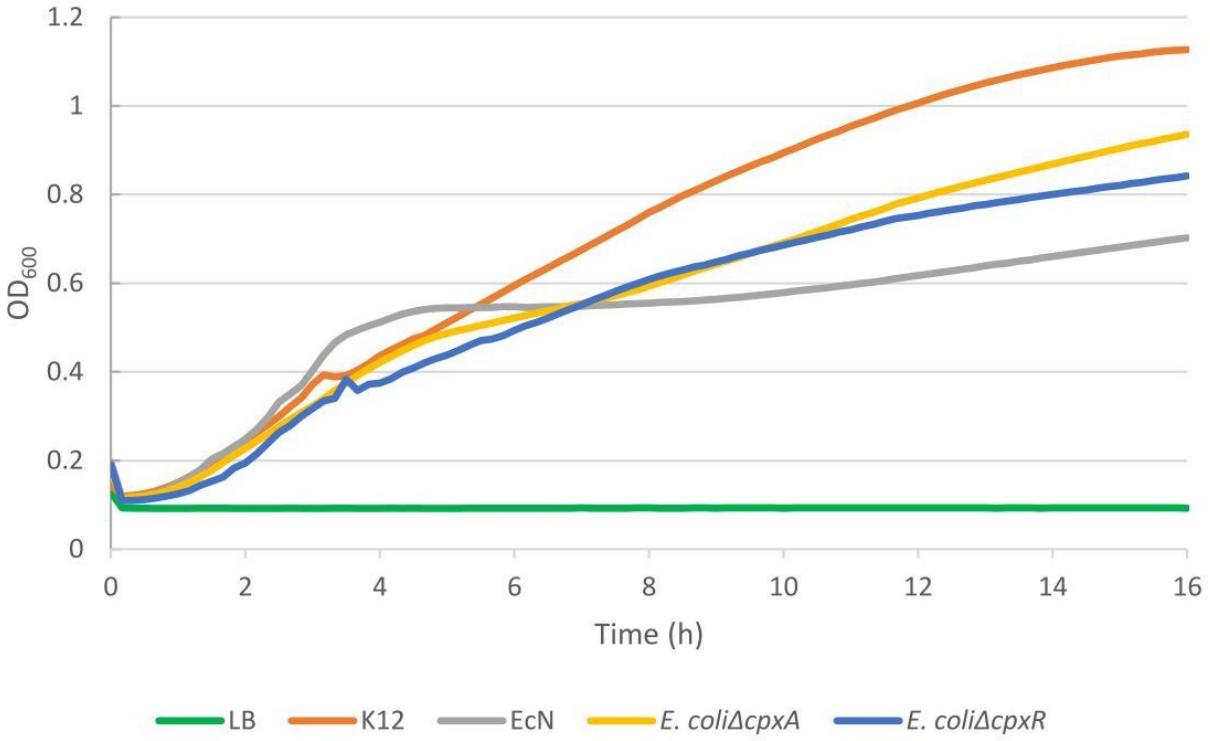

FIG. 5 Growth Curves of *E. coli* strains K-12, EcN, *E. coli ΔcpxA*, *E. coli ΔcpxR*. The strains were grown for 16 h at 37°C, shaking, and the OD600 was plotted for every 10 minute interval.

including initial inoculum concentration, temperature, aeration, growth media, and length of incubation (for specific conditions tested and results, see Fig. S1 in the supplemental material). Figure S1 shows that K12, which is the strain that showed the greatest amount of biofilm formation across all experimental conditions, exhibited minimal levels of biofilm formation in all experiments performed in 96-well plates. Fig. S3 demonstrates that a co-culture of K12 with EcN had a 2.3-fold decrease in K12 biofilm formation when compared to a K12 monoculture, which supports our hypothesis and agrees with previous findings (13). However, these results were not observed when we repeated this experiment while controlling for a potential evaporation bias (Fig. S4), a result of the well contents in the perimeter of the 96-well plate being prone to evaporation. Taken together, our findings suggest that optimization of growth conditions for biofilm formation in 96-well plates results in inconsistent data.

Air-liquid-solid interface allows for improved biofilm formation. Next, we decided to investigate if incubation in glass test tubes promotes biofilm development, and if this can lead to the development of a biofilm assay that allows for robust quantification of biofilm and downstream experiments using this assay. To achieve this, one plate-isolated colony from each of the four strains was used to inoculate glass test tubes with either 1 mL or 4 mL LB, using the same monoculture and co-culture conditions as described previously. These test tubes were then loosely-capped, incubated at 30°C for 72 h without shaking, adapted from (16), and stained and washed as described previously. By comparing biofilm formation in polystyrene 96-well plates vs glass test tubes (Fig. S1), we determined that the amount of biofilm formation is highest when bacterial cultures are incubated in loosely-capped glass test tubes with 1 mL LB, without shaking, at 30°C for 72 h. Our findings demonstrate that incubation in glass test tubes, when compared to polystyrene 96-well plates, resulted in a 1.6-fold increase in biofilm formation in the Δ*cpxR* monoculture, approximate 2-fold increases in the EcN monoculture and K12 and EcN co-culture, 2.6-fold increase in the K12 monoculture, and a 3.2-fold increase in the Δ*cpxA* and EcN co-culture (Fig. 6). The biofilms formed visible rings in the test tubes at the air-liquid-solid interface, which is at the location of the meniscus. The biofilm rings were visible before and after

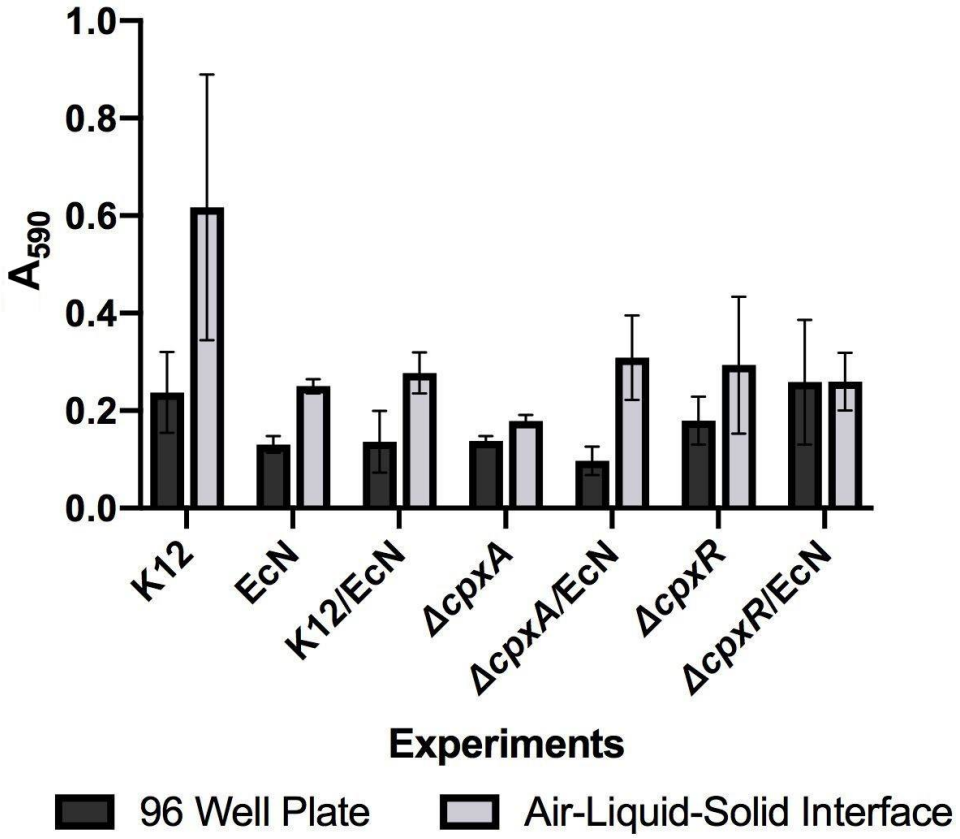

FIG. 6 Biofilm Expression (A590) of Strains Grown in 96-well plate versus 5 mL glass tubes. In the 96-well plates, the cultures were grown at 37°C for 96 h non-shaking. In the air-liquid-solid interface experiments, the cultures were grown in 1 mL LB at 30°C for 72 h non-shaking. The figure shows means of three technical replicates of each culture with the error bars indicating the standard deviation.

staining with crystal violet (Fig. 7). These rings, suggesting robust biofilm formation (16), were not observed in the Δ*cpxA* monoculture (Fig. 7) or in any of the bacterial cultures incubated in 96-well plates.

Air-liquid-solid interface experiments show a trend toward decreased biofilm formation in K12 when co-cultured with EcN. After observing that EcN may decrease biofilm formation in K12, Δ*cpxA,* and Δ*cpxR* in 96-well plates (Fig. S3), we wanted to examine if this was also the case for biofilms forming as rings on glass test tubes at the air-liquid-solid interface. Therefore, air-liquid-solid interface biofilm assays were conducted as described above with monocultures of K12, EcN, Δ*cpxA* and Δ*cpxR* and co-cultures of EcN and K12, EcN and Δ*cpxA,* and EcN and Δ*cpxR.* Results indicate that K12 exhibits the highest amount of biofilm formation, with an A590 value of 0.62, and that the co-culture of K12 and EcN shows an A590 value of 0.25, corresponding to approximately a 2.5-fold decrease in biofilm formation (Fig. 8). The K12 and EcN co-culture indicated a similar level of biofilm formation as the EcN monoculture, and this result is also observed when comparing the Δ*cpxR*/EcN and EcN monoculture (Fig. 8). The Δ*cpxA* monoculture shows the lowest level of biofilm formation, at an A590 value of 0.18, whereas the Δ*cpxA* and EcN monoculture shows an A590 value of 0.31, which corresponds to a 1.7-fold increase (Fig. 8). While these results are inconclusive for determining the effect of EcN-mediated biofilm inhibition in co-cultures with Δ*cpxA* and Δ*cpxR,* it suggests that EcN may decrease K12 biofilm formation in a co-culture.

DISCUSSION

In an attempt to elucidate the mechanism of Cpx-mediated biofilm inhibition in co-cultures with EcN, we first focused on optimizing growth conditions for assay development of

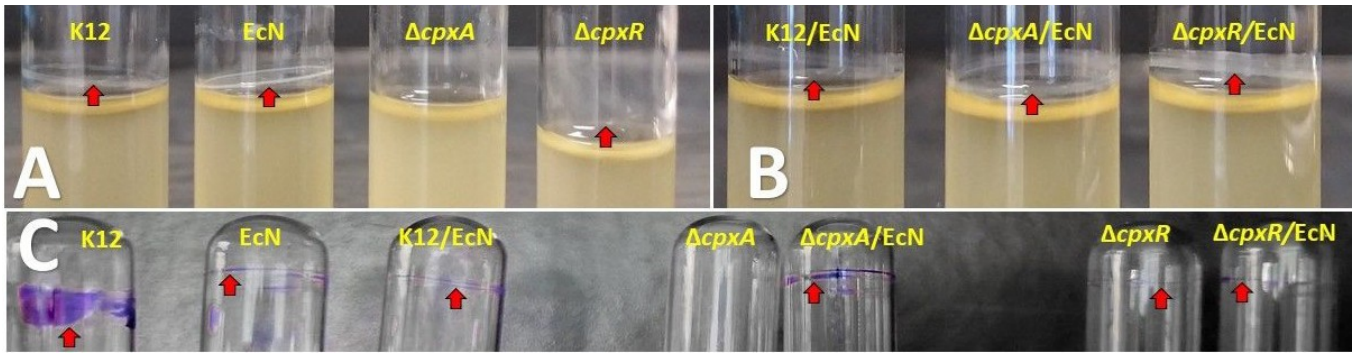

FIG. 7 Biofilm formation as rings in glass test tubes in 1 mL of LB, incubated at 30°C for 72 h. Arrows identify the location of the biofilm ring at the meniscus of the air-liquid-solid interface. Test tubes were held at an angle to clearly visualize the rings, thus slightly affecting the location of the meniscus relative to the test tube. (A) Biofilm rings were observed in all monocultures except Δ*cpxA*. (B) Biofilm rings are observed in all co-cultures. (C) Biofilm rings stained with 0.1% crystal violet. All conditions exhibited a purple ring of biofilm formation except the Δ*cpxA* monoculture.

biofilm formation, detection and quantification before performing the glass tube growth assay to explore the mechanism of Cpx-mediated biofilm inhibition in co-cultures with EcN.

Challenges in developing detectable amounts of biofilm in 96-well plates. After a series of optimization processes that included temperature, shaking, and seeding concentrations, we did not obtain consistent, observable biofilm expression in the 96-well plates. We expected, as demonstrated by previous findings, to see a decrease in biofilm formation when EcN is co-cultured with the K12 strain (13). We observed this trend in the LB 96 h first experiment and the air-liquid-solid interface experiment (Fig. S3 and 8); however, in the LB 96 h second experiment, no significant difference was observed between the different experimental groups (Fig. S4). Furthermore, the difference, compared between the K12 and the K12/EcN co-culture, was also insignificant (Fig. S3 and S4). We propose that the observation in our LB 96 h first experiment was due to an evaporation bias because of the fact that wells seeded at the perimeter of the plate (K12 monoculture and Δ*cpxR*/EcN co-culture) showed higher biofilm readings than those in the center of the plate. This may be caused by the aeration and low humidity within the 96-well plate after being left in the incubator for a longer period of time (96 h). Furthermore, the 96-well plate was incubated while shaking, which was not the case for previous work (13), and thus may have also decreased the ability of cells to form biofilms on the sides of the wells. This led to two follow-up experiments that were performed to resolve the evaporation bias. The first experiment, adapted from (13), yielded results that were statistically insignificant and showed high levels of variation, with absorbance values that were similar to the blank (Fig. S4). A possible explanation for such an observation is that we did not first transfer the enriched population into a medium with antibiotics added; thus, the result observed may be caused by the planktonic cells outcompeting the biofilm cells, or may be due to contamination from airborne bacteria during the incubation period. This is supported by the results of all experiment groups lying clearly within one standard deviation of one another (Fig. S4). In addition, plates were incubated at 37°C, which may further promote the growth of planktonic cells over biofilm cells. Overall, there were many challenges in developing detectable amounts of biofilm using 96-well plates, including competition with planktonic cells, evaporation bias, and growth conditions such as temperature and shaking during incubation.

Biofilm experiments with glass tubes sufficiently exhibit biofilm formation and shows EcN may be involved in Cpx pathway biofilm formation. In our final experiment, we observed sufficient biofilm formation from our co-culture experiments seeded in glass tubes, representing an improvement to the biofilm assay. The greatest amount of biofilm formation by K12, EcN, Δ*cpxA,* and Δ*cpxR* was observed in 1 mL of LB in glass test tubes at 30°C, without shaking, for 72 h. This setup eliminates the observed evaporation bias in

the 96-well plates since each bacterial culture was grown in its own test tube. In this experiment, there was a 2.5-fold decrease in biofilm in the K12/EcN co-culture compared to the K12 monoculture (Fig. 8). This result gives support to the trend observed in the LB 96 h first experiment despite the presence of evaporation bias (Fig. S3). Furthermore, it is in line with the results obtained by previous work as EcN is a strain that secretes DegP, which inhibits biofilm formation (13). Yet, no significant difference was observed between the Δ*cpxR* monoculture, and Δ*cpxA*/EcN and Δ*cpxR*/EcN co-cultures (Fig. 8). In addition, both Δ*cpxR* and Δ*cpxR*/EcN showed a 2.5 fold decrease in biofilm formation (Fig. 8), which was contrary to our model. Only the Δ*cpxA* monoculture result supported our model as it demonstrated a 3.5-fold decrease in biofilm formation, but we observed a 1.7-fold increase when co-cultured with EcN (Fig. 8). These data suggest that EcN may not be involved in the Cpx pathway; however, the observation that Δ*cpxA*/EcN showed significantly more biofilm formation than the Δ*cpxA* monoculture could indicate that experimental parameters may not have been fully optimized since expected results were either the co-culture showing no change in biofilm level (which supports our model) or a reduction in biofilm level (which refutes our model). Thus, further investigation should be performed to determine whether DegP may be involved in other pathway mechanisms within *E. coli*. Taken together, our findings suggest that EcN may reduce biofilm formation in K12, but the mechanism of biofilm inhibition may not be linked to the Cpx pathway, and that the biofilm assay and setup still requires further optimization.

Glass test tube assay allows for increased biofilm formation when compared to polypropylene or polystyrene 96-well plates. Over the course of several condition optimizations, our results suggest that *E. coli* forms biofilms on glass test tubes

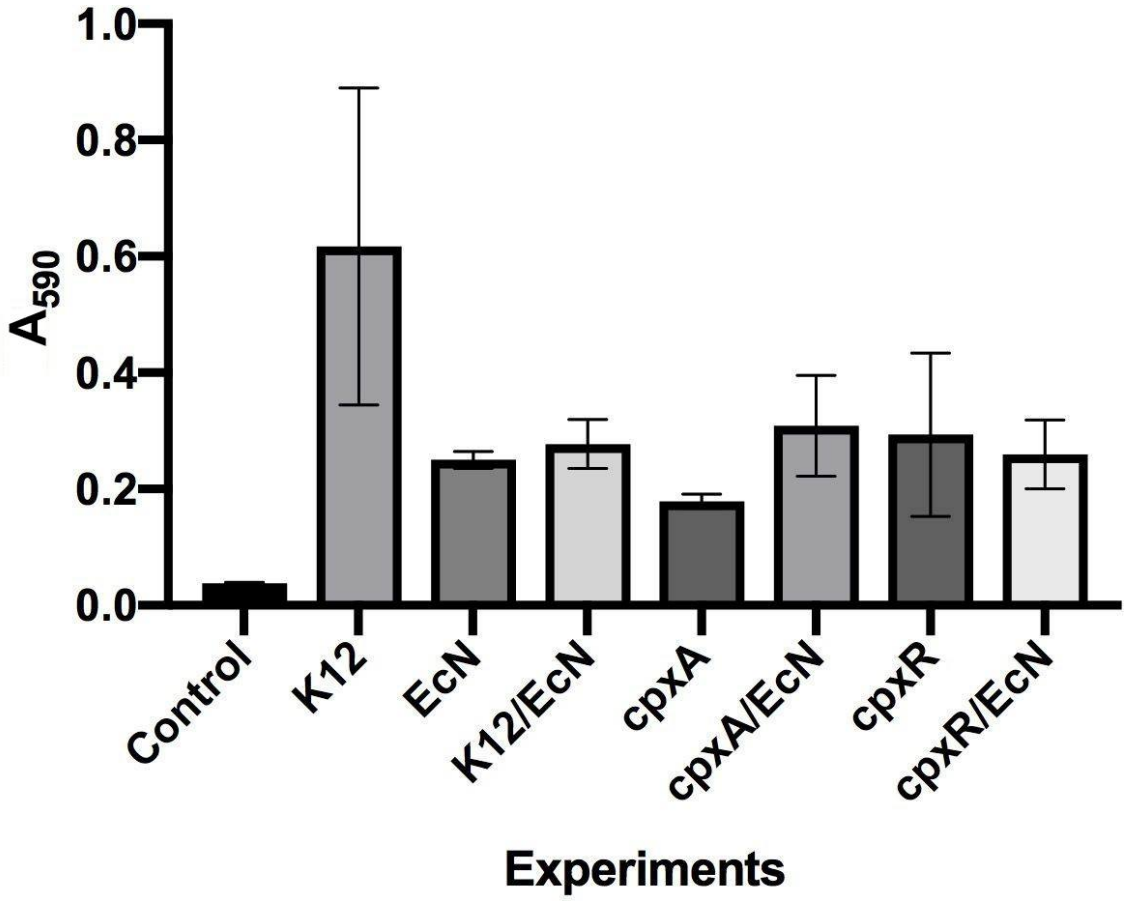

FIG. 8 Biofilm Expression (A590) of strains in glass tubes containing 1 mL culture. The strains were grown over 72 h at 30°C in glass tubes with the lid loosely capped. After crystal violet staining, the A590 was read of each culture. The bars show the mean of three technical replicates and the error bars show the standard deviation. The control was LB media.

preferentially to polystyrene or polypropylene 96-well plates. In order to compare the two materials, we used polypropylene 96-well plates and polystyrene 96-well plates in one experiment (Fig. S5). Cultures from both plates did not yield overtly visible biofilm rings in the wells; however, in the glass tubes, K12, EcN, Δ*cpxA*, Δ*cpxR*, and co-cultures produced strongly visible biofilm rings (Fig. 7). This may be largely attributed to the presence of a larger air-liquid solid interface in the glass test tube assay, as well as larger overall culture volume. In addition, literature has suggested that some microorganisms, such as *Staphylococcus aureus*, form biofilm that attach more readily to hydrophilic residues like glass (17). Biofilm formation by *Bacillus cereus* also exhibit higher affinity for glass compared to plastic (18). In future experiments, it might be prudent to continue growing our cultures in glass tubes, but also test metal surfaces as well, as one study has shown that *B. cereus* biofilm forms up to 3-fold better on metal compared to glass (18). Our results from the 96-well plates and glass tube experiments show that the glass tube assay allows for enhanced biofilm growth compared to polystyrene or polypropylene 96-well plates.

The air-liquid-solid surface interface may enhance biofilm formation. Our results suggest that the air-liquid-solid interface may be required for the formation of biofilm in *E. coli* strains. The ring of biofilm cells observed at the meniscus region inside the test tube suggests that conditions for optimal biofilm formation in the 4 strains tested are at the air-liquid-solid surface interface, where oxygen abundance from the air above and nutrient availability from the growth medium below are at the highest concentration. This is in agreement with previous findings which reported that certain bacterial biofilm cells may grow to a greater density at the air-liquid-solid or air-liquid interface when compared to submerged biofilm cells, which colonize areas away from the surface of the growth medium (19). Enhanced growth at the air-liquid-solid interface may be facilitated by the adhesive properties of the cells to the interface due to the physical adhesion of the biofilm - a result from interactions between lipopolysaccharide, cellulose fibers, and attachment factors (19). In addition, the hydrophobic nature of this complex structure (19) may further encourage biofilm development at the air-liquid-solid interface, rather than colonizing at or below the surface of the LB medium.

Another factor that we hypothesized to play a role in allowing for biofilm formation was the ratio of the surface area to volume of the growth medium. We compared the levels of biofilm formation of bacterial cultures grown in glass test tubes with 1 mL of LB with those grown in 4 mL of LB (data not shown). Although the latter condition represents growth conditions with a lower surface area to volume ratio, both groups exhibited similar levels of biofilm formation. Thus, we conjecture that there is a minimum ratio of surface area to volume that must be met in order for sufficient biofilm formation to occur. Should that minimum not be reached (in the case of the cultures in the 96-well plates), then biofilm formation may not occur. Therefore, our results suggest that the surface area to volume ratio of the liquid growth medium does potentially affect the amount of biofilm formation.

Conclusions Based on our findings, we conclude that EcN may have inhibitory effects on the development of K12 biofilm in liquid co-cultures. We have demonstrated that biofilm development is enhanced when incubated in glass test tubes vs polypropylene or polystyrene 96-well plates, and that this may be largely due to the presence of a larger air-liquid-solid interface in glass test tubes. Although our developed assay suggests EcN may reduce biofilm formation in K12, it is inconclusive if the EcN inhibitory effects are due to interactions with the Cpx pathway.

Future Directions A key future experiment is to determine conditions and consistently reproduce results that demonstrate detectable levels of biofilm formation as seen in the 1 mL glass test tube experiment. Once the optimal conditions have been set for K12 and EcN, and a baseline for expected biofilm production established, the experiments with Δ*cpxA* and Δ*cpxR* can be repeated for more conclusive results.

Though the K12/EcN co-culture was shown to have a decreased amount of biofilm formation, the large deviation within each treatment suggests the need for a greater number of biological and technical replicates in future experiments. This may also allow us to

identify whether extracellular DegP is involved in biofilm inhibition within the Cpx pathway as the current data does not allow us to draw any conclusion regarding its involvement.

As we have been using variations of biofilm assays throughout our study, further investigation into each method would elucidate if there are any additional pitfalls that were not taken into account, such as the evaporation bias when we used the 96-well plates to perform the crystal violet biofilm assay. Duplicates of experiments that have produced prominent results should be performed to verify replicability in our observed results.

Given the uncertainty regarding EcN and its involvement with the Cpx pathway in regulating biofilm formation in *E. coli*, we propose further experiments should be performed to confirm if our model is likely. An *E. coli* Δ*cpxP* strain may be used in future experiments as CpxP interacts directly with DegP (8). Further, the experiments can be repeated using EcN with the *degP* gene knocked out, allowing us to see if biofilm formation in K12 will be restored to normal levels in the co-culture experimental group. These additional experiments will allow us to obtain more conclusive observations about whether DegP and the Cpx pathway are involved in the inhibition of biofilm formation.

Finally, purification of EcN containing media should be performed to verify the presence of DegP. Isolated DegP can be then used for future experiment to corroborate whether DegP is sufficient for biofilm inhibition, and to further test the model when Δ*cpxA* and Δ*cpxR* are grown in media containing purified DegP. Both deletion strains should not show a significant difference with or without the addition of DegP.

ACKNOWLEDGEMENTS

We would like to extend our gratitude towards Dr. David Oliver and Mihai Cirstea for their guidance and support throughout our research project. We also want to thank the media room for providing us with equipment, and other teams from the class for their collaboration. Lastly, we would like to acknowledge the Department of Microbiology and Immunology and for providing the funding to support our research.

CONTRIBUTIONS

Alex Fung, Anderson Li, Helen Lin and Vivian Li contributed equally to the overall design and execution of the experiments. All authors contributed equally to the preparation of this manuscript.

REFERENCES

1. **Bjarnsholt T.** 2011. SpringerLink ebooks - Biomedical and Life Sciences. Biofilm Infections. 1st ed. New York: Springer
2. **López D, Vlamakis H, Kolter R.** 2010. Biofilms. Cold Spring Harbor Perspectives in Biology, 2: a000398. doi:10.1101/cshperspect.a000398.
3. **Serra DO, Richter AM, Hengge R.** 2013. Cellulose as an Architectural Element in Spatially Structured *Escherichia coli* Biofilms. J Bacteriol doi: 195:5540-5554.
4. **Markova JA, Anganova EV, Turskaya AL, Bybin VA, Savilov ED**. Regulation of *Escherichia coli* Biofilm Formation (Review). Applied Biochemistry and Microbiology 2018;54:1-11.
5. **Otto K, Silhavy TJ.** 2002. Surface sensing and adhesion of *Escherichia coli* controlled by the Cpx-signaling pathway. Proc Natl Acad Sci USA 99:2287-2292.
6. **Rendueles O, Ghigo J**. 2012. Multi-species biofilms: how to avoid unfriendly neighbors. FEMS Microbiol Rev 36:972-989.
7. **Mika F, Hengge R**. 2014. Small RNAs in the control of RpoS, CsgD, and biofilm architecture of *Escherichia coli*. RNA Biol doi:10.4161/rna.28867.
8. **Isaac DD, Pinkner JS, Hultgren SJ, Silhavy TJ.** 2005. The extracytoplasmic adaptor protein CpxP is degraded with substrate by DegP. Proc Natl Acad Sci USA 102: 17775-17779. doi:10.1073/pnas.0508936102.
9. **Buelow, DR, Raivio, TL**. 2005. Cpx signal transduction is influenced by a conserved N-terminal domain in the novel inhibitor CpxP and the periplasmic protease DegP. J Bacteriol 187:6622-6630. doi: 187/19/6622.
10. **Ge X, Wang R, Ma J, et al.** 2014. DegP primarily functions as a protease for the biogenesis of β-barrel outer membrane proteins in the Gram-negative bacterium *Escherichia coli*. FEBS J 281:1226-1240.
11. **Soltes GR, Martin NR, Park E, Sutterlin HA, Silhavy TJ.** 2017. Distinctive Roles for Periplasmic Proteases in the Maintenance of Essential Outer Membrane Protein Assembly. J Bacteriol doi:10.1128/JB.00418-17.

12. **MacRitchie, DM, Acosta, N, Raivio, TL**. 2012. DegP is involved in Cpx-mediated posttranscriptional regulation of the type III secretion apparatus in enteropathogenic *Escherichia coli*. Infect Immun 80:1766-1772. doi: 10.1128/IAI.05679-11.
13. **Fang K, Jin X, Hong SH.** 2018. Probiotic *Escherichia coli* inhibits biofilm formation of pathogenic *E. coli* via extracellular activity of DegP. Sci Rep 8: 1-12. doi:10.1038/s41598-018-23180-1.
14. **Groban ES, Clarke EJ, Salis HM, Miller SM, Voigt CA**. 2009. Kinetic Buffering of Cross Talk between Bacterial Two-Component Sensors. J Mol Biol 390:380-393.
15. **Prigent-Combaret C, Vidal O, Dorel C, Lejeune P**. 1999. Abiotic Surface Sensing and Biofilm-Dependent Regulation of Gene Expression in *Escherichia coli*. J Bacteriol 181:5993-6002.
16. **Sutrina SL, Callender S, Grazette T, Scantlebury P, O'Neal S, Thomas K, Harris DC, Mota-Meira M.** 2018. The quantity and distribution of biofilm growth of *Escherichia coli* strain ATCC 9723 depends on the carbon/energy source. Microbiology 10.1099/mic.0.000745.
17. **Lee J, Bae Y, Lee S, Lee S.** Biofilm Formation of *Staphylococcus aureus* on Various Surfaces and Their Resistance to Chlorine Sanitizer. J Food Sci 2015;80: M2279-M2286.
18. **Kwon M, Hussain MS, Oh DH**. 2017. Biofilm formation of *Bacillus cereus* under food-processing-related conditions. Food Sci Biotechnol 26:1103-1111.
19. **Koza A, Hallett PD, Moon CD, Spiers AJ.** 2009. Characterization of a novel air-liquid interface biofilm of *Pseudomonas fluorescens* SBW25. Microbiology 155: 1397-140